
Supplementary information

**Maladaptation, migration and extirpation
fuel climate change risk in a forest tree
species**

In the format provided by the
authors and unedited

Supplemental Materials

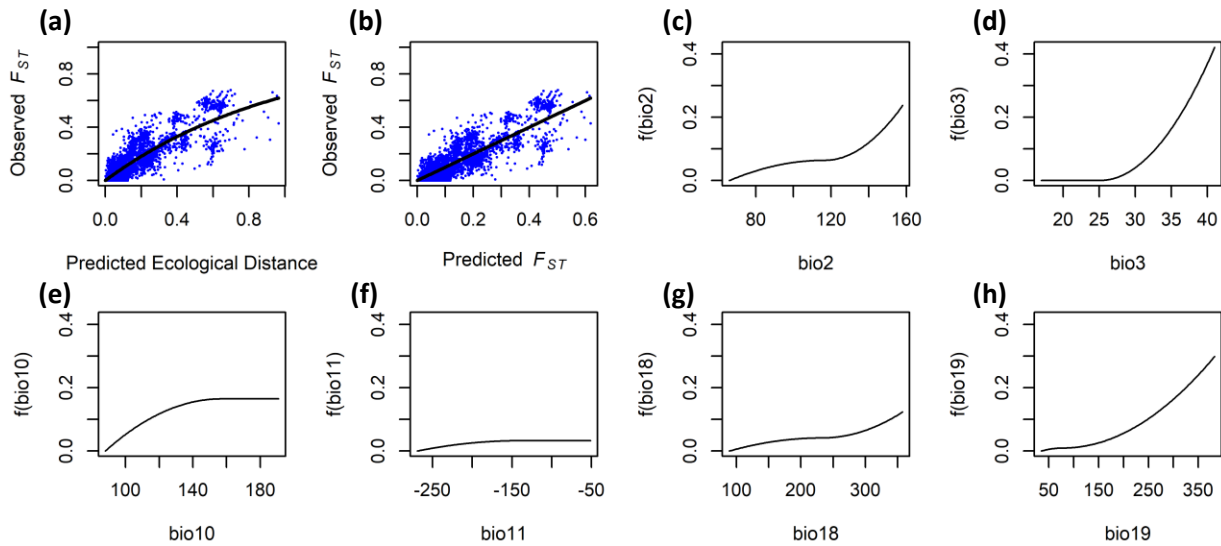


Fig. S1. (a & b) Generalized dissimilarity model (GDM) fit and (c-h) climatic response plots. GDM was fit to F_{ST} of 75 SNPs in the *Populus* flowering time network across 81 range-wide balsam poplar populations (bio2: mean diurnal range; bio3: isothermality; bio10: mean summer temperature; bio11: mean winter temperature; bio18: summer precipitation; bio19: winter precipitation). ‘Observed F_{ST} ’ is the calculated F_{ST} between pairs of populations, and ‘Predicted F_{ST} ’ is the predicted value from the GDM. Predicted ecological distance is the sum of transformed climate predictors between pairs of populations. I-spline functions transforming climate predictors (denoted as ‘f()’ on the y-axes) are shown in c – h. b shows the fit of the model, where the black line is a 1:1 line.

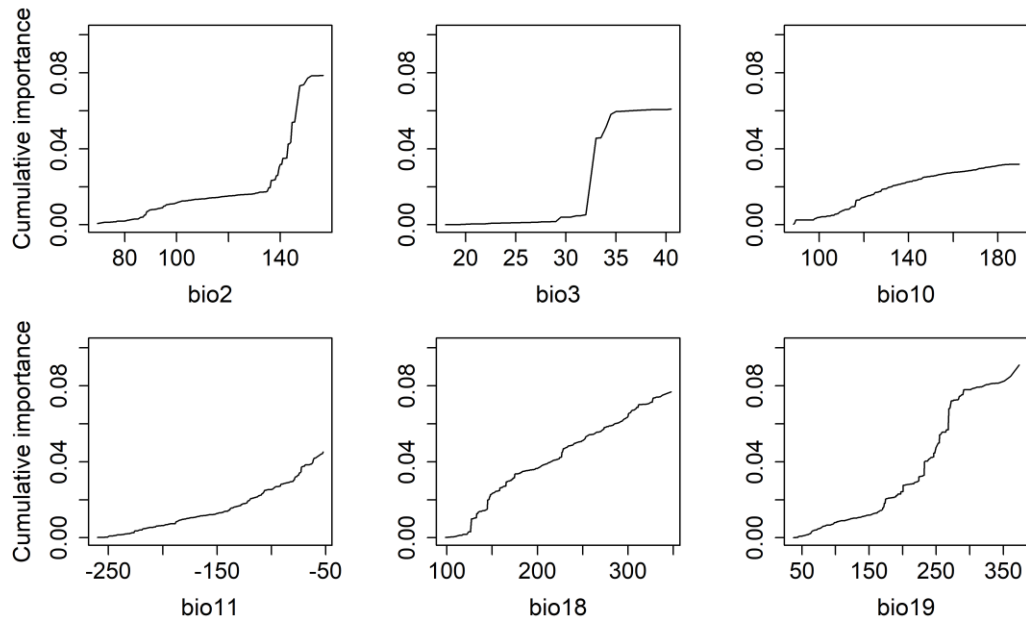


Fig. S2. Aggregate turnover functions for Gradient Forest for each climate variable (bio2: mean diurnal range; bio3: isothermality; bio10: mean summer temperature; bio11: mean winter temperature; bio18: summer precipitation; bio19: winter precipitation). The maximum height of each curve indicates the amount of turnover in allele frequencies along each climate variable, and the relative importance of each climate variable in explaining allele frequency turnover across 81 balsam poplar populations.

(a)

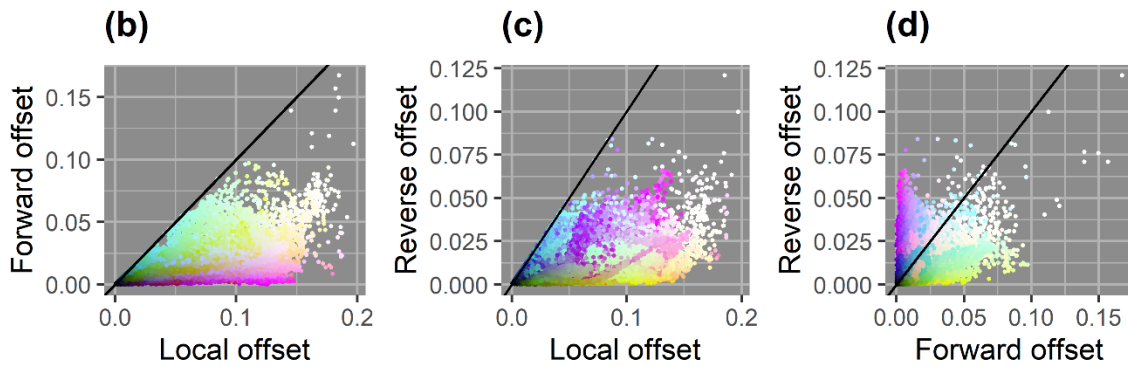
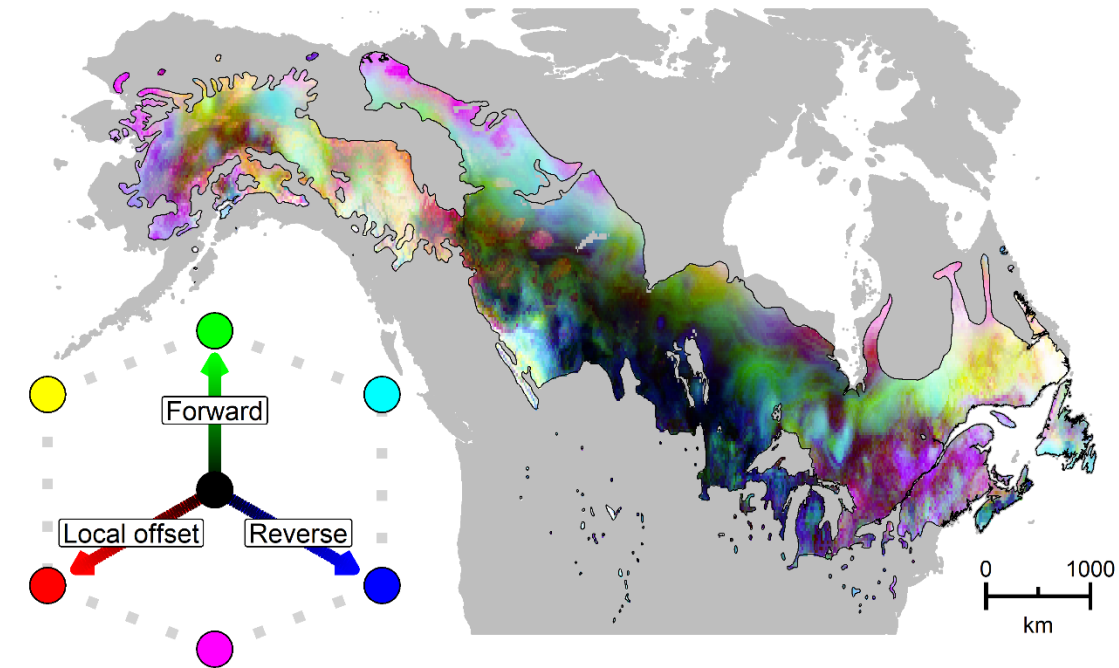


Fig. S3. Red-green-blue map of local (red), forward (green), and reverse (blue) offsets. Offset values were calculated from generalized dissimilarity models throughout the range of balsam poplar for 2070 and RCP 4.5. Brighter cells, closer to white, have relatively high values along each of the three axes while darker cells, closer to black, have relatively lower values. (b-d) Bivariate scattergrams of (a), with 1:1 lines. Individual maps used in (a) are shown in Extended Fig. 3.

(a)

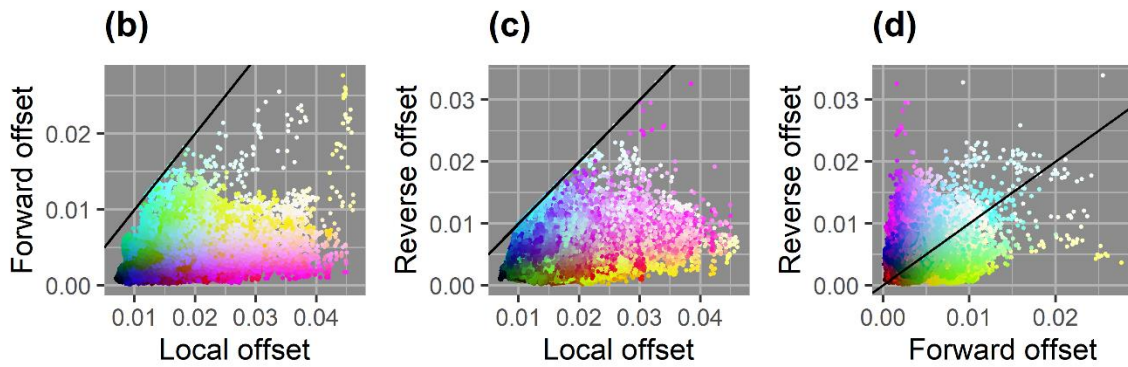
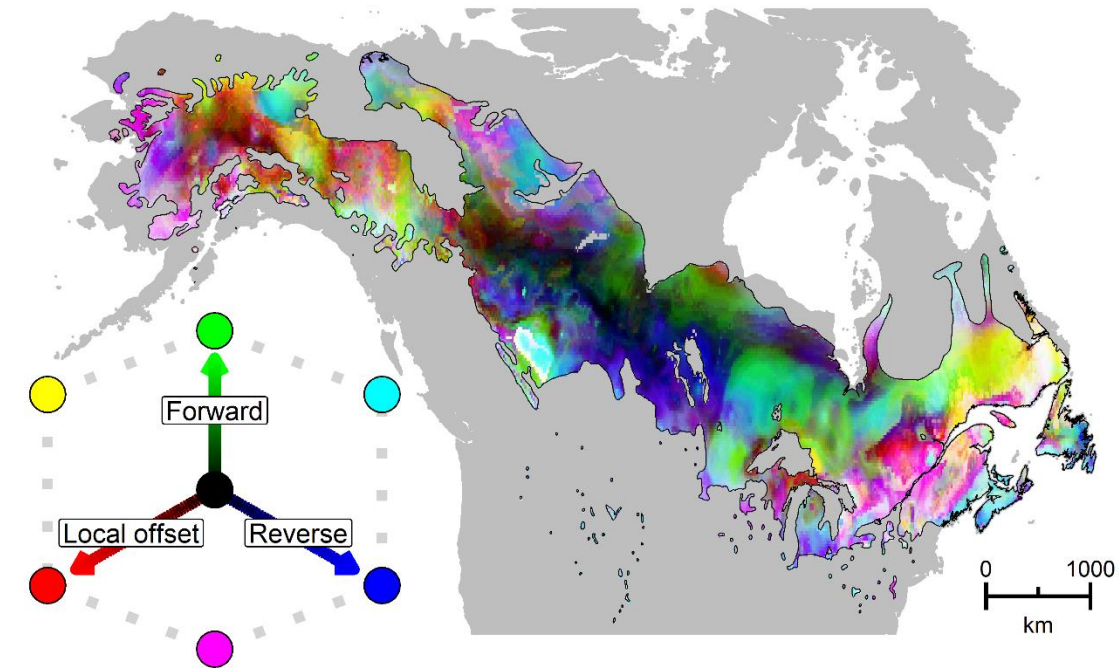
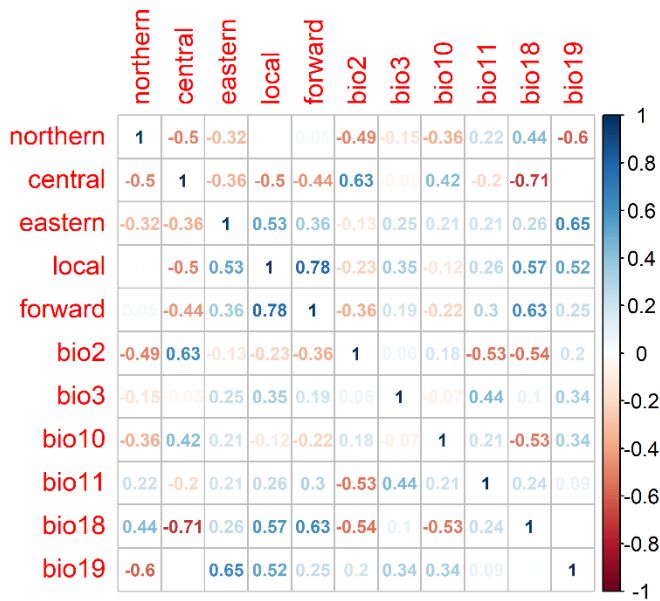


Fig. S4. Red-green-blue map of local (red), forward (green), and reverse (blue) offsets. Offset values were calculated from Gradient Forest throughout the range of balsam poplar for 2070 and RCP 4.5. Brighter cells, closer to white, have relatively high values along each of the three axes while darker cells, closer to black, have relatively lower values. (b-d) Bivariate scattergrams of (a), with 1:1 lines. Individual maps used in (a) are shown in Extended Fig. 4.

(a)



(b)

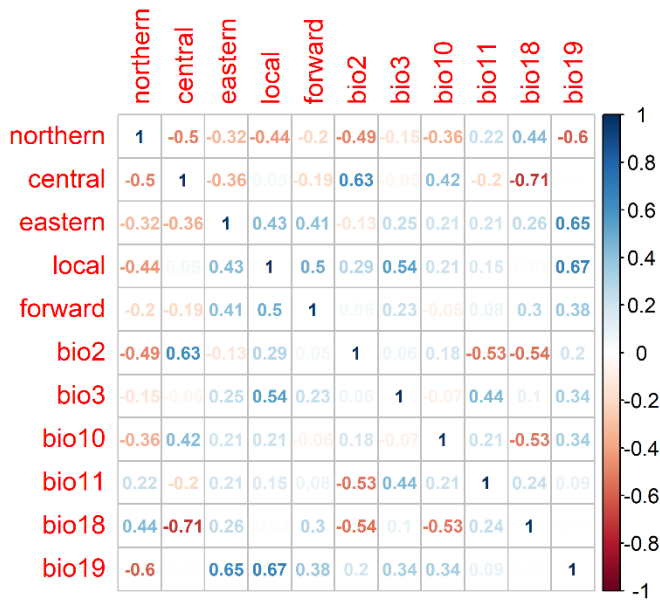
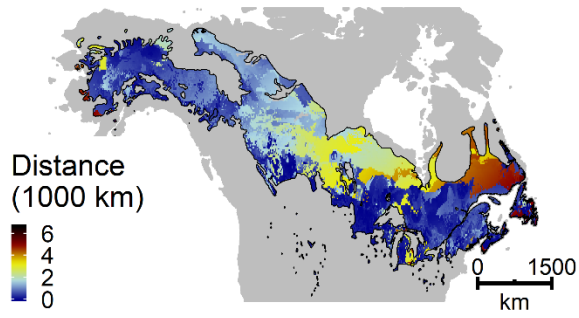


Fig. S5. Spearman rank correlation between local and forward offsets from (a) generalized dissimilarity model and (b) Gradient Forest, climatic shifts, and ancestry coefficients. Climatic shifts were calculated as future climate (2070, RCP 8.5) minus current climate, for each climate

variable (bio2: mean diurnal range; bio3: isothermality; bio10: mean summer temperature; bio11: mean winter temperature; bio18: summer precipitation; bio19: winter precipitation). Ancestry coefficients represent the relative affiliation of each population to three genetic clusters in balsam poplar's range ('northern', 'central' and 'eastern' clusters). Ancestry coefficients are meant to represent neutral population structure, and were collected from Gougherty et al. (2020) for 85 balsam poplar populations. Panels (a) and (b) differ only in the model used to calculate local and forward offsets (generalized dissimilarity models, and Gradient Forest, respectively) – ancestry coefficients, and climate shifts are identical.

(a)



(b)

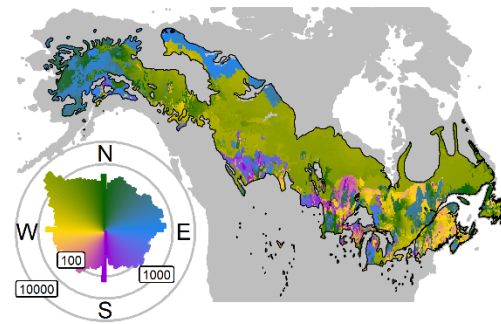
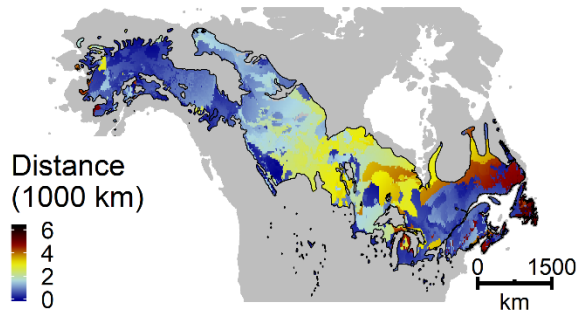


Fig. S6. Distance and initial bearing to locations that minimizes forward offset. (a) Distance and (b) initial bearing were calculated from the focal cell to the location in future North American climate (2070, RCP 4.5) that minimizes predicted F_{ST} from a generalized dissimilarity model. Polar histogram in (b) shows the log10 number of cells in each bearing bin.

(a)



(b)

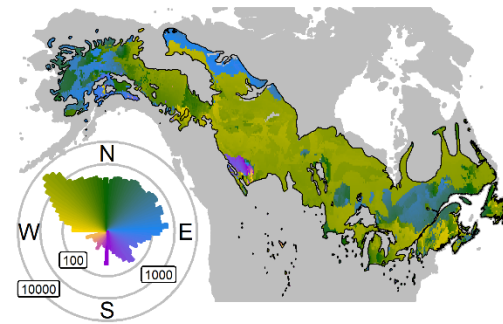


Fig. S7. Distance and initial bearing to locations that minimizes forward offset. (a) Distance and (b) initial bearing were calculated from the focal cell to the location in future North American climate (2070, RCP 4.5) that minimizes predicted offset from a Gradient Forest model. Polar histogram in (b) shows the log₁₀ number of cells in each bearing bin.

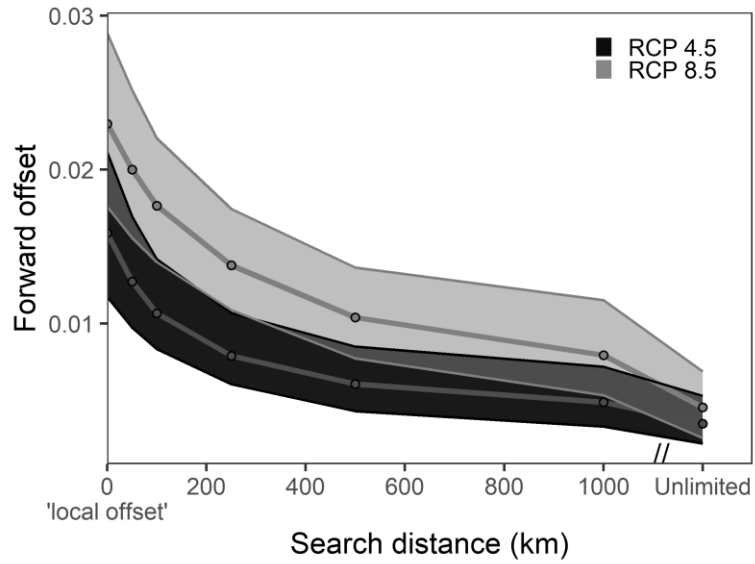


Fig. S8. Relationship between maximum allowable migration distance (i.e., search distance) and minimized forward offset from Gradient Forest for 2070. Bands extend between the 25th and 75th percentiles, and points are median values.

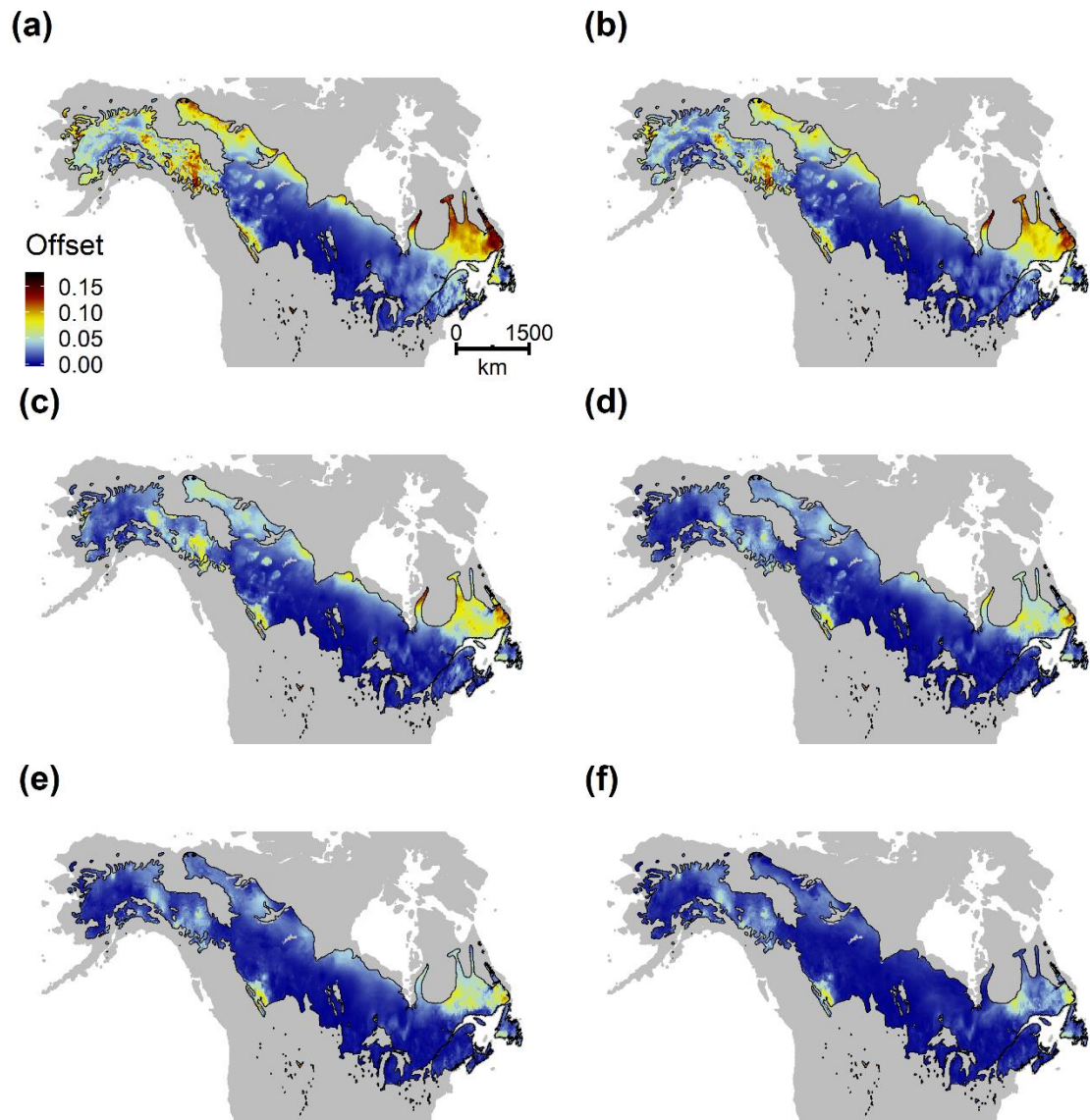


Fig. S9. Effect of search distance on forward offset from generalized dissimilarity models for RCP 4.5 in 2070. Distance classes included (a) 50 km, (b) 100 km, (c) 250 km, (d) 500 km, (e) 1000 km, and (f) unlimited.

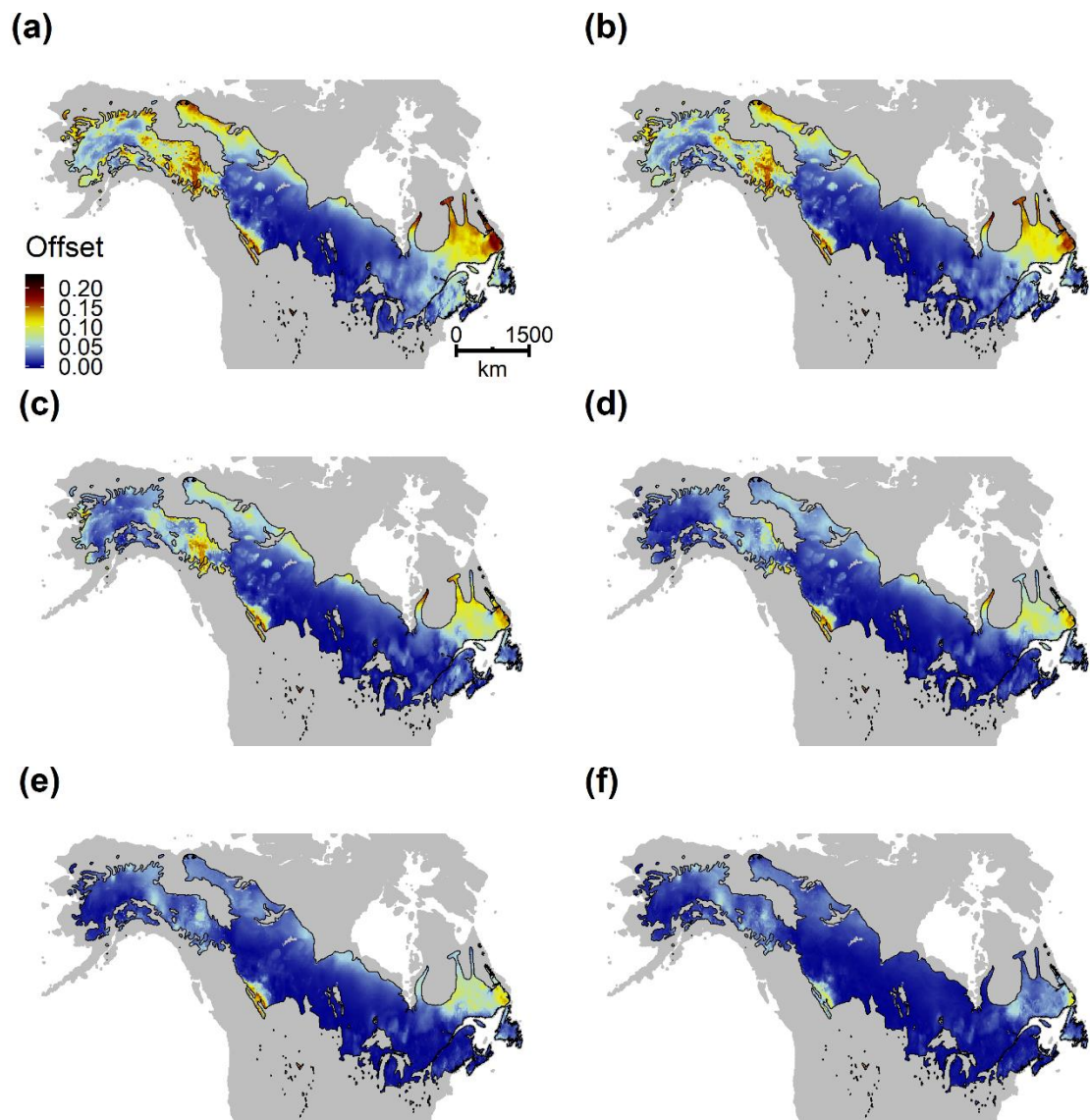


Fig. S10. Effect of search distance on forward offset from generalized dissimilarity models for RCP 8.5 in 2070. Distance classes included (a) 50 km, (b) 100 km, (c) 250 km, (d) 500 km, (e) 1000 km, and (f) unlimited.

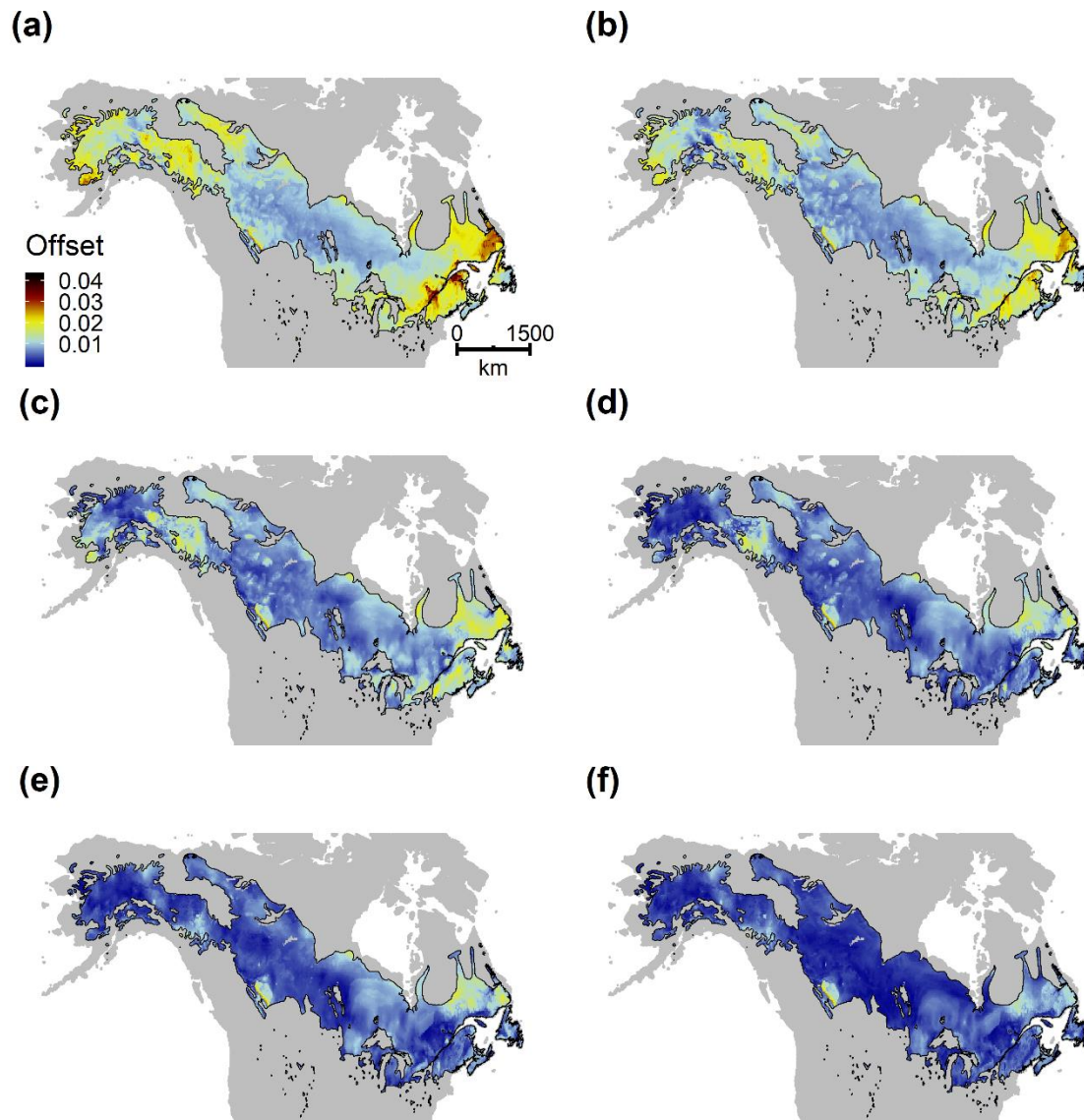


Fig. S11. Effect of search distance on forward offset from Gradient Forest for RCP 4.5 in 2070. Distance classes included (a) 50 km, (b) 100 km, (c) 250 km, (d) 500 km, (e) 1000 km, and (f) unlimited.

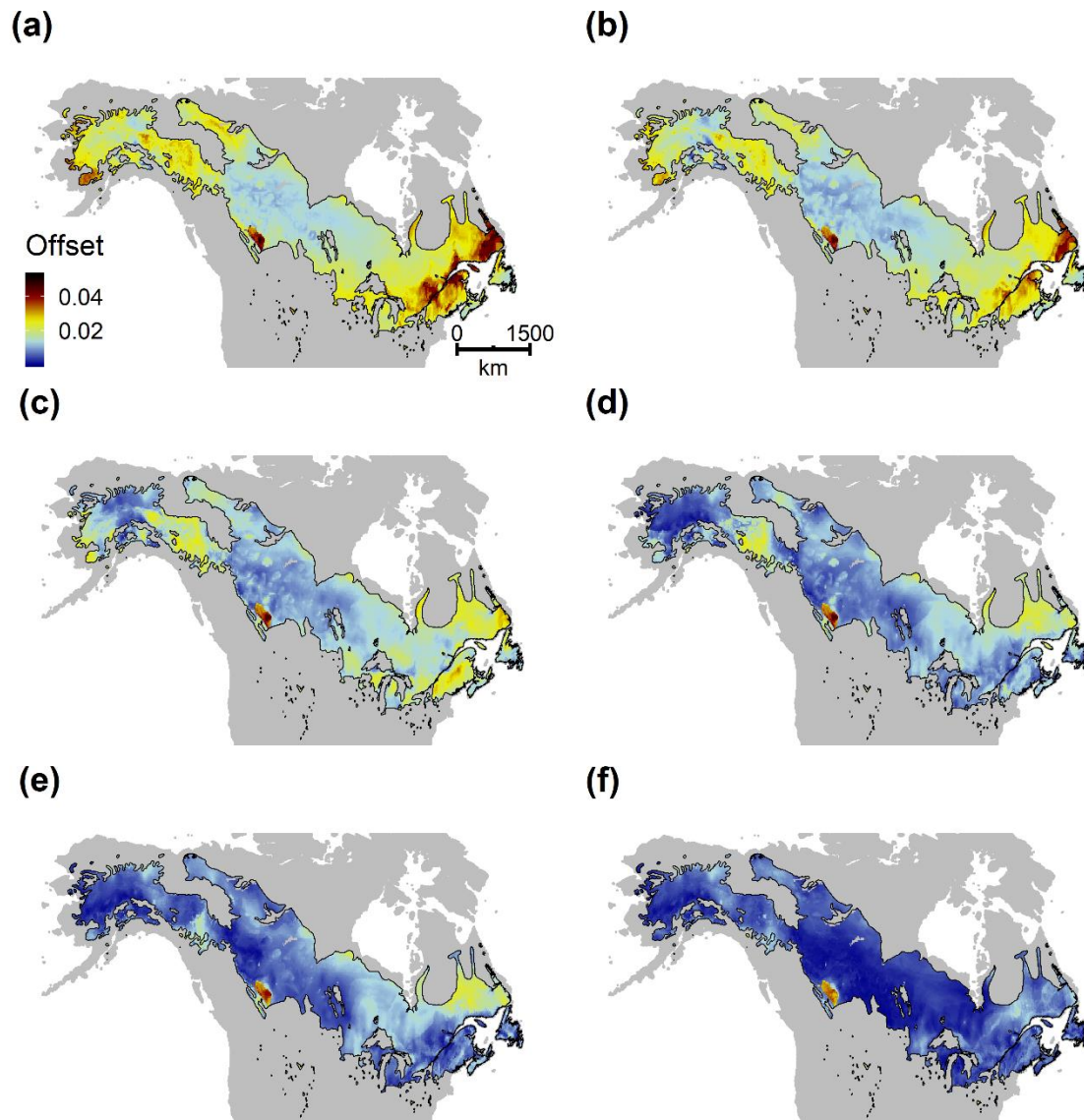


Fig. S12. Effect of search distance on forward offset from Gradient Forest for RCP 8.5 in 2070. Distance classes included (a) 50 km, (b) 100 km, (c) 250 km, (d) 500 km, (e) 1000 km, and (f) unlimited.

Table S1. Flowering time genes and number of SNPs used in Gradient Forest and generalized dissimilarity models.

| Gene | Gene ID | Annotation | No. SNPs |
|-------------------------------------|---------|----------------------------|----------|
| ABA insensitive-1B | ABI1B | Abscisic acid | 2 |
| ABA insensitive-1D | ABI1D | Abscisic acid | 3 |
| ABA insensitive-1D | ABI3 | Abscisic acid | 2 |
| Casein kinase-2 subunit β 3.4 | CKB3.4 | Peripheral circadian clock | 2 |
| Constans-1 | CO1 | Downstream target | 6 |
| Constans-2 | CO2 | Downstream target | 3 |
| Cryptochrome-1.1 | CRY1.1 | Photoreceptor | 5 |
| Cryptochrome-1.2 | CRY1.2 | Photoreceptor | 2 |
| Early bolting in short days | EBS | Downstream target | 2 |
| Early flowering-3 | ELF3 | Peripheral circadian clock | 15 |
| Gigantea-2 | GI2 | Peripheral circadian clock | 2 |
| Gigantea-5 | GI5 | Peripheral circadian clock | 10 |
| Heme oxygenase-1.1 | HY1.1 | Photoreceptor | 1 |
| Heme oxygenase-1.2 | HY1.2 | Photoreceptor | 2 |
| Heme oxygenase-2.1 | HY2.1 | Photoreceptor | 2 |
| Heme oxygenase-2.2 | HY2.2 | Photoreceptor | 1 |
| Leafy | LFY | Downstream target | 1 |
| Phytochrome-B1 | PHYB1 | Photoreceptor | 1 |
| Phytochrome-B2 | PHYB2 | Photoreceptor | 2 |
| Phytochrome interacting factor-3 | PIF3 | Photoreceptor | 3 |
| Flowering locus T-1 | PtFT1 | Downstream target | 2 |
| Terminal flowering-1.1 | TFL1.1 | Downstream target | 1 |
| Timing of cab-1 | TOC1 | Central circadian clock | 2 |
| ZEITLUPE-2.9 | ZTL2.9 | Photoreceptor | 3 |

Table S2. Variable importance from generalized dissimilarity model. Importance is calculated as the decrease in deviance explained when the variable is permuted. Permutations fit indicates the number of iterations when the model is successfully fit when variables are permuted.

| Climate variable | Variable ID | Importance (%) | Significance | Permutations fit (of 100) |
|-------------------------|-------------|----------------|--------------|---------------------------|
| Mean diurnal range | bio2 | 1.308 | 0.03 | 100 |
| Isothermality | bio3 | 4.389 | < 0.01 | 99 |
| Mean summer temperature | bio10 | 4.593 | < 0.01 | 100 |
| Mean winter temperature | bio11 | 0.271 | 0.17 | 100 |
| Summer precipitation | bio18 | 2.075 | < 0.01 | 100 |
| Winter precipitation | bio19 | 10.912 | < 0.01 | 100 |